

DOI: <https://doi.org/10.30898/1684-1719.2023.12.17>

УДК: 537.9

COLLECTIVE NATURE OF LOW-TEMPERATURE PHOTOCONDUCTION AND CONDUCTION IN THE PEIERLS CONDUCTOR ORTHORHOMBIC TaS_3

V.E. Minakova, S.V. Zaitzev-Zotov

Kotelnikov IRE RAS
125009, Russia, Moscow, Mokhovaya str., 11, b.7

The paper was received November 29, 2023.

Abstract. This work summarizes the results of series of works devoted to the study of the mechanisms of low-temperature conduction and photoconduction in the Peierls conductor orthorhombic TaS_3 (o- TaS_3). We used the tools we discovered to change the relationship between the single-particle and collective components of low-temperature photoconduction and conduction in o- TaS_3 – illumination and uniaxial stretching of the sample. Using them, we were able to separate single-particle and collective contributions and show that the collective contribution dominates both low-temperature conduction ($T \lesssim 100$ K) and low-temperature photoconduction ($T \lesssim 45$ K). In addition, the discovered analogy between the influence of illumination and stretching on low-temperature conduction and photoconduction made it possible to establish the dimension of charge density wave (CDW) pinning in samples of different cross-sections at low temperatures. It was found that for all samples, including bulk ones, one-dimensional pinning is observed at temperatures $T < 40$ K, and it also has a collective character.

Key words: charge-density wave, non-linear conduction, collective conduction, solitons, photoconduction.

Financing: The research was carried out within the framework of the state assignment of the Kotelnikov IRE RAS No. 122042000064-1.

Corresponding author: Minakova Valeria Evgen'evna, mina_cplire@mail.ru

Introduction

The appearance of a charge density wave (CDW) in quasi-one-dimensional (q-1D) conductors with decreasing temperature T leads to the emergence of unusual properties of these compounds at temperatures below the Peierls transition temperature, T_P [1, 2]. The most striking of them is the presence of a collective mechanism of current transfer, caused mainly by CDW sliding in small electric fields, E , exceeding the threshold value, E_T , which leads to strong nonlinear conduction. In addition, nonlinear CDW excitations solitons can also contribute to the collective conduction. The possibility of their existence in Peierls conductors was theoretically considered in [3, 4], and experimentally demonstrated in the study of NbSe₃ using both scanning tunneling microscopy [5] and in an interlayer tunneling experiment [6].

In *o*-TaS₃ ($T_P \approx 220$ K), already in the first work [7], it was discovered that the activation dependence of the Ohmic conduction $G(T)$ in the longitudinal direction changes at low temperatures ($T \lesssim T_P/2$), and in the transverse direction remains unchanged over the entire temperature range, namely: the activation energy of longitudinal conduction at low T , Δ_L , decreases approximately by half compared to the activation energy $\Delta_P \approx 800$ K at $T_P/2 \lesssim T < T_P$. The results were presumably associated with the appearance of solitons, whose activation energy is lower than the activation energy of quasiparticles.

The ability to distinguish the contributions of single-particle and collective CDW excitations to low-temperature Ohmic conduction appeared with the discovery of tools for changing the relationship between the quasiparticle and soliton components of conduction, such as illumination of the sample and its uniaxial strain. In the first case, it is possible to increase the concentration of nonequilibrium quasiparticles by exciting them over the Peierls gap, which leads to an increase in Ohmic conduction, that is, to the appearance of photoconduction [8]. In the second case, additional solitons appear

because strain increases the degree of deviation of the CDW wave vector q [9] from fourfold commensurability, to which it approaches with decreasing temperature [10, 11].

1. Effect of illumination

By studying photoconduction in o -TaS₃ [12], it is possible to separate the contribution of electrons and holes excited over the Peierls gap to low-temperature Ohmic conduction. The experimental methods and data processing are described in [12]. The results are shown in Fig. 1, which shows the temperature dependence of dark Ohmic conductance $G(T)$ (upper curve) and a set of temperature dependences of photoconductance $g(T)$, measured under modulated illumination at different illumination levels W . In the dependence $G(T)$ below $T_P = 210$ K one can see high-temperature and low-temperature regions with activation energies $\Delta_P = 800$ K $\Delta_L = 400$ K, respectively. The temperature dependences of photoconductance $g(T)$ have a characteristic maximum at $T \approx 60$ K, which, as was shown in [12], separates the regions of linear and quadratic recombination of nonequilibrium carriers produced by illumination. The black straight lines in the $g(T)$ dependences correspond to activation laws with a single activation energy $\Delta_\tau = 1250$ K. When each $g(T)$ curve is normalized to the corresponding light intensity value W , they all “collapse” in the high-temperature part into one, which proves the existence of a linear recombination regime in this temperature region. This activation law $g(T)$ is determined by the activation dependence of the lifetime of nonequilibrium current carriers $\tau \propto \exp(\Delta_\tau/kT)$, which explains why photoconduction is observed only at relatively low temperatures $T \lesssim 77$ K. The circles indicate points at which the concentration of photo-excited current carriers is equal to the equilibrium concentration of carriers responsible for the photoresponse for the case of stationary photoconduction; at these points, the photoconductance $g(T)$ is equal to the dark single-particle conductance $G_{qp}(T)$. The straight line passing through them is the activation law with activation energy $\Delta_{qp} = 1250$ K. This straight line visualizes the single-particle contribution to low-temperature conduction. Since at $T < 100$ K the activation energy of single-particle

conduction Δ_{qp} is significantly greater than the activation energy of low-temperature Ohmic conduction Δ_L , the single-particle conduction channel in nominally pure and spatially homogeneous *o*-TaS₃ samples cannot be determinative at low T . It is shunted by an additional non-single-particle mechanism of low-temperature conduction associated with CDW degrees of freedom, and therefore low-temperature Ohmic conduction has a collective origin.

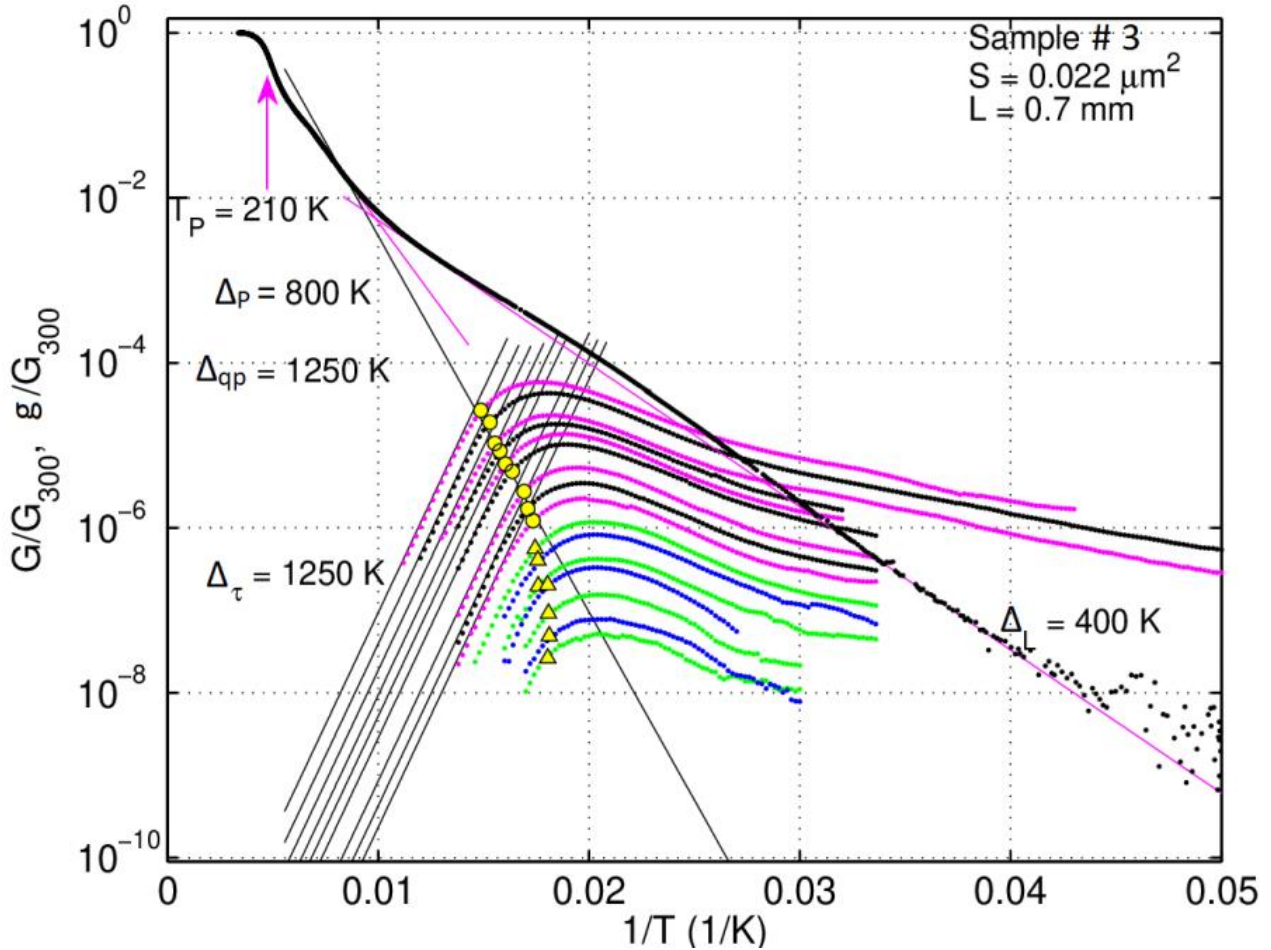


Fig. 1. The upper curve (black dots) is the dark temperature dependence of the Ohmic conductance of *o*-TaS₃ $G(T)$. The arrow indicates the Peierls transition temperature $T_P = 210$ K. The colored straight lines are activation laws describing the high-temperature part of Ohmic conductance with activation energy $\Delta_P = 800$ K and its low-temperature part with $\Delta_L = 400$ K. The set of curves in the lower part of the figure shows the temperature dependences of photoconductance $g(T)$ at different intensities of light W (top to bottom) 10; 4; 1.8; 1; 0.5; 0.28; 0.077; 0.038; 0.02; 0.0082; 0.005; 0.0024; 0.0014; 0.00062; 0.00031; 0.00019 mW/cm². The parallel black straight lines correspond to activation laws with activation energies $\Delta_\tau = 1250$ K. The circles indicate points corresponding to the dark single-particle conductance $G_{qp}(T)$. The straight line passing through them — the activation law with activation energy $\Delta_{qp} = 1250$ K — visualizes the dark single-particle conductance $G_{qp}(T)$.

When studying the spectral characteristics of *o*-TaS₃ [13, 14], no direct evidence of the existence of solitons was found. But in a few samples, when studying the photoconduction spectra [14], intragap states were discovered near the edge of the Peierls gap, depending on E and T , and their possible nature was associated with collective CDW excitations. These are the samples in which a “plateau” was observed on $G(T)$ – a region of weakly varying conductance separating conductance regions with high and low activation energies. The nature of the plateau is not fully known. But, in our opinion, such $G(T)$ dependences are inherent in samples subjected to special or random strain (see below).

Table 1. Parameters of the studied thin samples

Sample number	Resistance at $T = 300$ K, R_{300} (kOhm)	Sample length, L (μm)	Cross-sectional area, S (μm^2)
# 1	430	340	0.002
# 2	33.2	310	0.028
# 3	95	700	0.022
# 4	30.6	630	0.062
# 5	19.5	910	0.14
# 6	7	400	0.17

Not only the conduction increases under illumination, but also the value of the threshold field E_T [8] (see Fig. 2). The effect of illumination on E_T was first discovered in blue bronze $\text{K}_{0.3}\text{MoO}_3$ [15], but the results were misinterpreted. Later, the discovery and study of photoconduction in relatively thin samples of *o*-TaS₃ [8] (see Table 1) made it possible to discover a correlation between the values of the threshold field for the onset of CDW sliding and the Ohmic conductance $E_T \propto G^{1/3}$ (see inset to Fig. 2). The increase in E_T upon illumination is explained by a decrease in the CDW elastic modulus due to changes in screening conditions with the appearance of nonequilibrium current carriers [8]. The exponent $\alpha = 1/3$ indicates the case of one-dimensional (1D) pinning [16] (which corresponds to the sizes of the studied samples). For two samples (# 1 and #5), a series of dependences of the conductance, $G = I/V$, on the voltage across

the sample, V , (see Fig. 2), from which the dependences of the threshold field on the Ohmic conductance $V_T(G_T)$ were extracted, were systematically measured at different T over a wide temperature range.

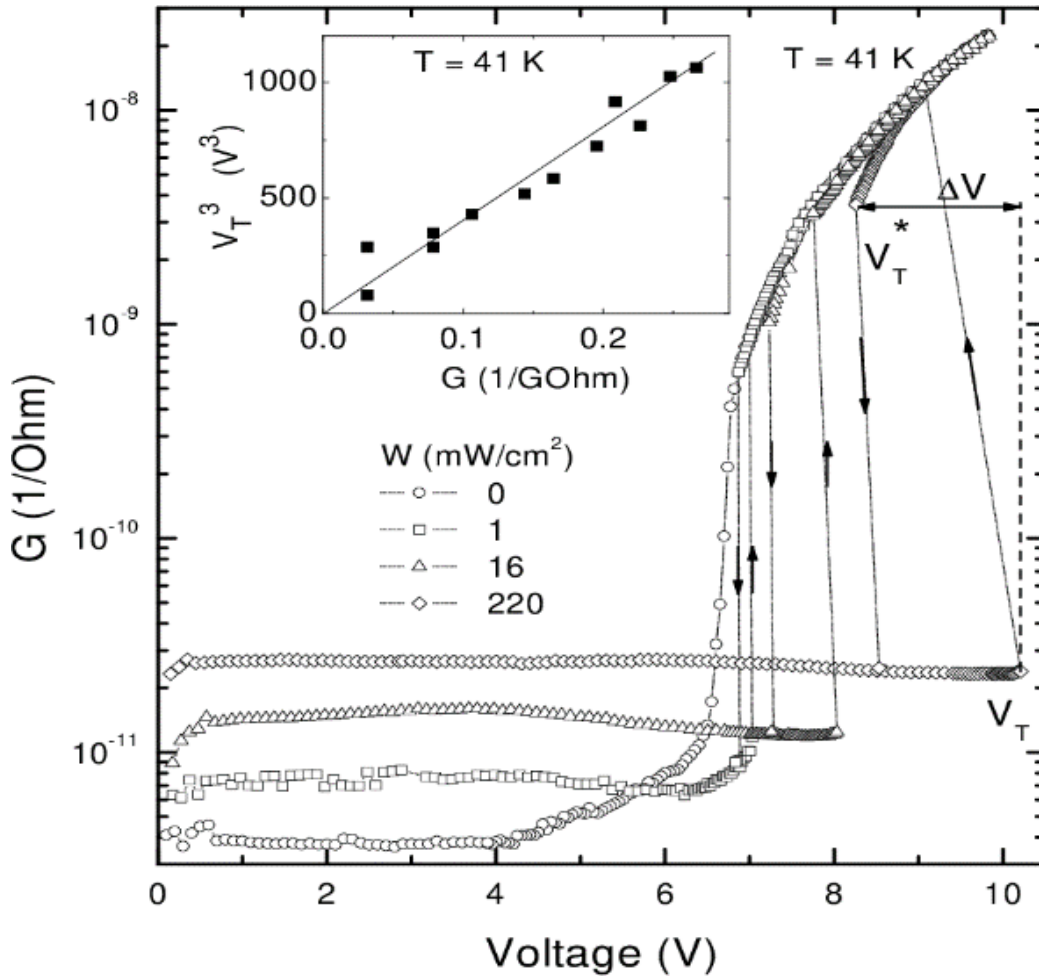


Fig. 1. Conductance of sample #1, $G=I/V$, as a function of sample voltage, V , at various illumination levels W at $T = 41$ K [8]. The inset shows the relationship between threshold voltage, V_T , and Ohmic conductance G (measured at $V = 100$ mV) at different W .

This made it possible to obtain a series of $V_T(G_T)$ dependences for these samples at different T (Fig. 3) and to see that the exponent α for these samples does not change throughout the entire temperature range studied, including the region $T > 40$ K [17]. For the other four samples, a series of $G(V)$ dependencies were studied only at several T and the $V_T(G_T)$ relationship was not tested in detail for them.

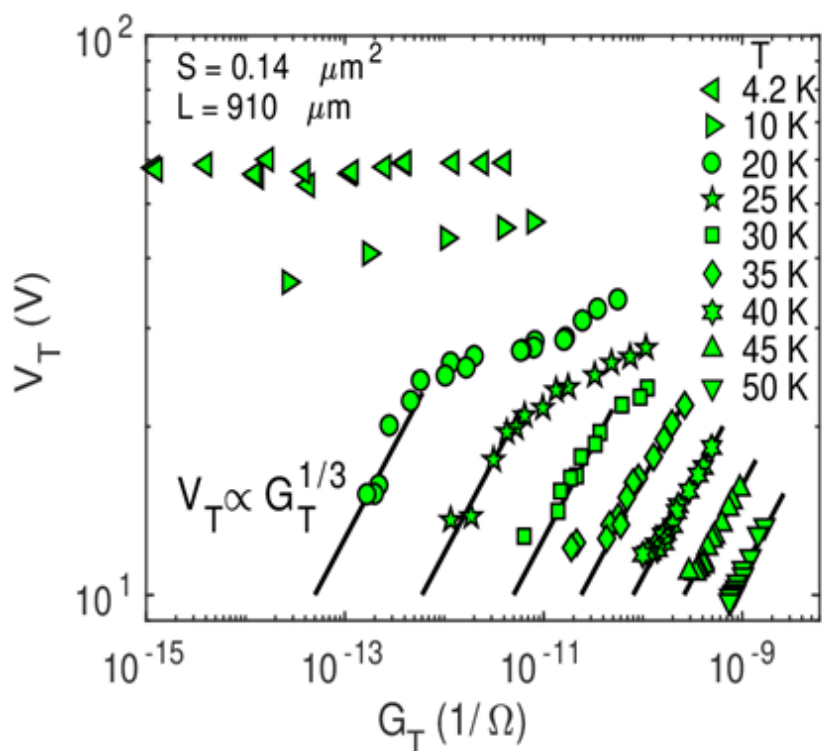


Fig. 2. Relationship between threshold voltage, V_T , and Ohmic conductance, $G_T = I_T/V_T$, at various T for sample #5 [17]. Straight lines correspond to the power law $E_T \propto G^{1/3}$.

2. Effect of strain

Before the appearance of work [18], the effect of strain on various properties of o -TaS₃ was studied in many works [19, 20, 9, etc.], but all of them were carried out at temperatures above 77 K. In work [18], a study of the effect of strain was carried out not only on low-temperature conductance (both Ohmic and nonlinear), but also on photoconductance, which is also observed only at $T \lesssim 80$ K. Comparison of the temperature and field dependences of low-temperature conductance and photoconductance of different segments of a single sample with different values of strain made it possible to show that the contribution from collective current carriers (most likely solitons) also predominates in low-temperature photoconduction ($T \lesssim 45$ K). In addition, they are also involved in changing the nature of CDW pinning. A detailed description of the structure under study, created on the basis of a high-quality o -TaS₃ crystal, the method of its manufacture and the experimental technique are described in [18].

This four-terminal structure is shown schematically in the inset of Fig. 4. The structure contains segment B with a specially created strain $\epsilon \approx 0.5\%$ and segment A, which serves as a comparison sample; no strain was specially applied to it. The conductances of the unstrained and strained segments are denoted $G_A(T)$ and $G_B(T)$, respectively, and the photoconductances are $g_A(T)$ and $g_B(T)$, respectively. All data are normalized to the corresponding room temperature conductances, G_{300} . In this case, such normalization is analogous to normalization by the length of the sample. The text below always refers to the normalized values of G and g .

Figure 4 shows the temperature dependences of the dark Ohmic conductance of the unstrained and strained segments of the sample, $G_A(T)$ and $G_B(T)$, respectively. At $100 \text{ K} \lesssim T < T_P$, the activation energies of both conductances are close to 850 K. A noticeable difference between the curves, $\delta G(T) = G_B(T) - G_A(T)$, appears at $T \gtrsim 70 \text{ K}$ in the plateau region connecting areas with high and low activation energies, the latter slightly differ from each other. With decreasing T , the increase in excess Ohmic conductance $\delta G(T)$ caused by strain leads to the fact that at low T the value of G_B exceeds G_A by an order of magnitude.

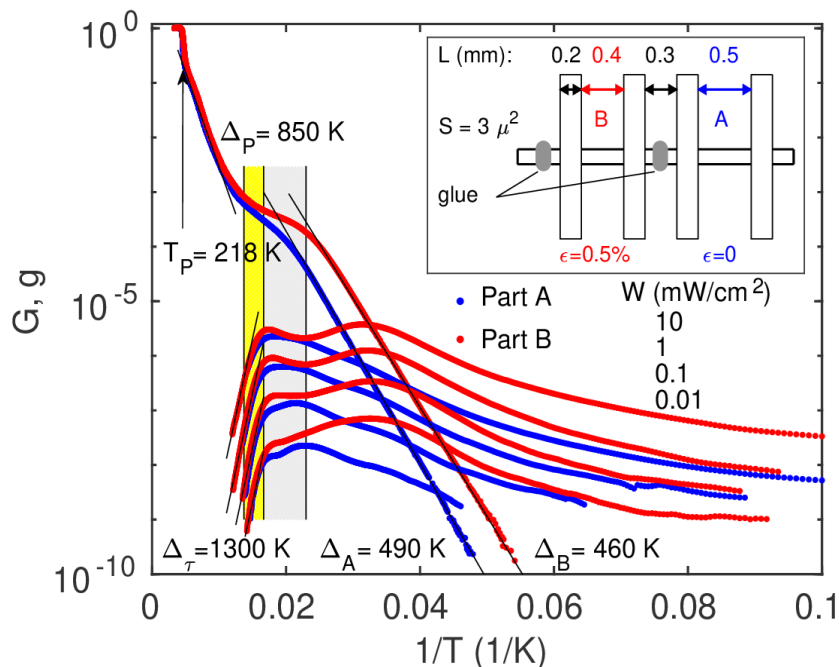


Fig. 3. Temperature dependences of normalized dark Ohmic conductances $G_A(T)$ and $G_B(T)$ (upper blue and red curves, respectively) and photoconductances $g_A(T)$ and $g_B(T)$ at different light intensities W (lower blue and red sets of curves, respectively) [18]. In the gray zone, the type of CDW pinning changes; in the yellow zone, a sharp change in $E_T(T)$ is observed. The inset shows a scheme of the structure under study.

The lower part of Figure 4 shows the temperature dependences of the photoconductances of the segments at different illumination levels W . For segment A, the observed behavior of $g_A(T)$ is usual: a sharp activation increase in photoconductance up to $T \approx 60$ K, then a smooth decrease with decreasing T . For the strained segment B, one can see a qualitative change in the curves: a new maximum appears at $T \approx 30$ K. As a result, at $T \lesssim 30$ K, a tenfold excess of $g_B(T)$ over $g_A(T)$ is observed for all W . Above $T \approx 45$ K, the difference between $g_A(T)$ and $g_B(T)$ becomes barely noticeable. In the region of activation dependence, the curves practically coincide.

Figure 5 shows the dependence of conductance $G=I/V$ on the electric field. For segment A they have a normal appearance. When strained, additional conductance $\delta G(T)$ appears already at $E \rightarrow 0$, i.e., Ohmic conductance increases. In addition, E_T also increases; the sharpest increase in E_T is observed in the range $60 \text{ K} \lesssim T \lesssim 70 \text{ K}$. One can see that $E_{TB} > E_{TA}$ for all T . Thus, in its manifestations, the strain effect is in many ways analogous to the effect of illumination.

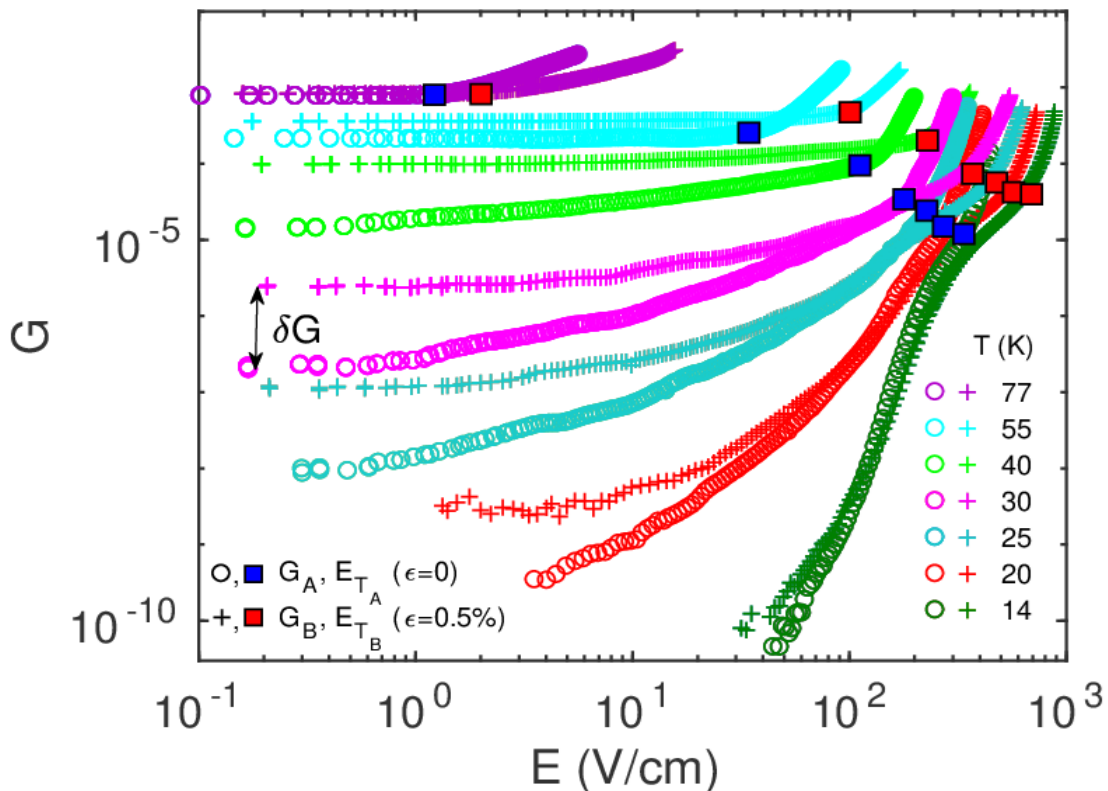


Fig. 5. Dependences of normalized conductances on the electric field for both sample segments $G_A(E)$ (circles) and $G_B(E)$ (crosses) at different T . Squares mark the values of E_{TA} (blue) and E_{TB} (red).

Field dependences of photoconductance without strain $g_A(E)$, presented in Fig. 6 have the usual form [21]. The onset of a sharp decrease in $g_A(E)$, is caused by the acceleration of carrier recombination with the onset of CDW motion at E_{TA}^* [8] (where E_{TA}^* is the threshold field for the onset of CDW motion in segment A under illumination). Strain leads to an increase in photoconductance already at $E \rightarrow 0$. In addition, E_{TB}^* also increases.

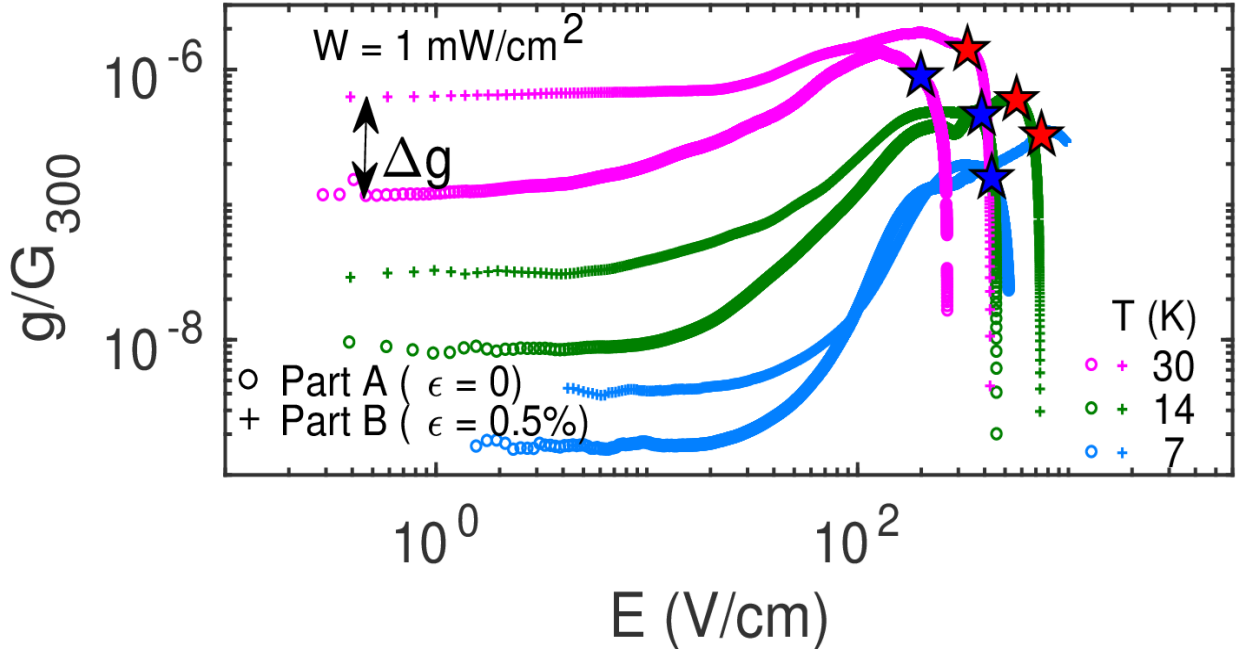


Fig. 4. Dependences of photoconductances on the electric field for both sample segments $g_A(E)$ (circles) and $g_B(E)$ (crosses) at low T . Stars mark the values E_{TA}^* (blue) and E_{TB}^* (red).

A detailed analysis of the results obtained [18] shows that at low T , the increase in photoconductance caused by strain is proportional to the change in conductance. As was shown in [12], during collisional recombination, which occurs in unstrained o -TaS₃ samples [12], an increase in the carrier concentration at T , $W = \text{const}$ should accelerate relaxation, reducing photoconduction. In our case, the effect is the opposite – strain leads to a consistent increase in conductance and photoconductance: in Fig. 4, all red curves are above the corresponding blue curves at $T \lesssim 60$ K. The difference becomes especially noticeable at $T \lesssim 45$ K.

The effect can be explained by analogy with [12], if we assume that the contribution to photoconduction, as well as to conduction, consists of two components:

nonequilibrium quasiparticles (electrons and holes) excited over the Peierls gap, and nonequilibrium solitons. Since in conduction, with decreasing T , the type of majority carriers changes from quasiparticle to soliton [12] due to the lower activation energy of solitons than quasiparticles, it is logical to assume that in photoconduction, solitons will play a dominant role at low T . And a significant increase in excess solitons under strain, due to an increase in the degree of CDW incommensurability [9], will lead to an even greater low-temperature dominance of the soliton contribution to both conduction and photoconduction, which is consistent with experiment. Thus, photoconduction, like conduction, can be divided into high-temperature photoconduction at $60 \lesssim T \lesssim 77$ K and low-temperature photoconduction at $T \lesssim 45$ K. The first is carried out by nonequilibrium quasiparticles; the laws of collisional recombination work for it. The second has a collective origin with its own laws. Therefore, it is quite appropriate to call the high-temperature maximum of photoconductance a quasiparticle peak, and the low-temperature maximum a soliton peak. It was reported in [22] that photoexcitation of nonequilibrium electrons and holes can also change the concentration of solitons and thereby make a collective contribution to photoconduction, which can be considered as “collective photoconduction.” Apparently, in the absence of strain, such collective photoconduction is too small and “sinks” against the background of single-particle photoconduction. Strain increases the contribution of collective photoconduction, making it comparable to the single particle contribution.

3. Analogy between strain and illumination

The analogy between the effects of strain and illumination reported in [18] made it possible to obtain both the $E_T(G)$ dependence at different T and the $\alpha(T)$ dependence for the sample under study. To do this, we used (where possible) four different values of threshold fields – E_{TA} , E_{TB} , E_{TA}^* , E_{TB}^* and the corresponding values of Ohmic conductances G_A , G_B , G_{A+g_A} , G_{B+g_B} , (see Fig. 7). One can see that the exponent α remains constant at low T , increases in the temperature range $45 \lesssim T \lesssim 60$ K, after which it does not change again. The inset shows the dependence $\alpha(T)$. The value

$\alpha = 1/3$ (dashed line) corresponds to 1D pinning, and $\alpha = 3$ (dash-dotted line) corresponds to three-dimensional 3D pinning [16]. Note that in the region $30 < T < 55$ K (see Fig. 7), the values of α were obtained in two ways – from measurements of the effect of strain on both conductance and photoconductance, and the values of α in both cases practically coincide. Since both the appearance of photoconduction and its change upon strain application result in a change in total conduction, such a coincidence of α means that for a change in conduction, it does not matter how additional current carriers were generated. And this confirms our assumption that both conduction and photoconduction have a collective nature at low temperatures.

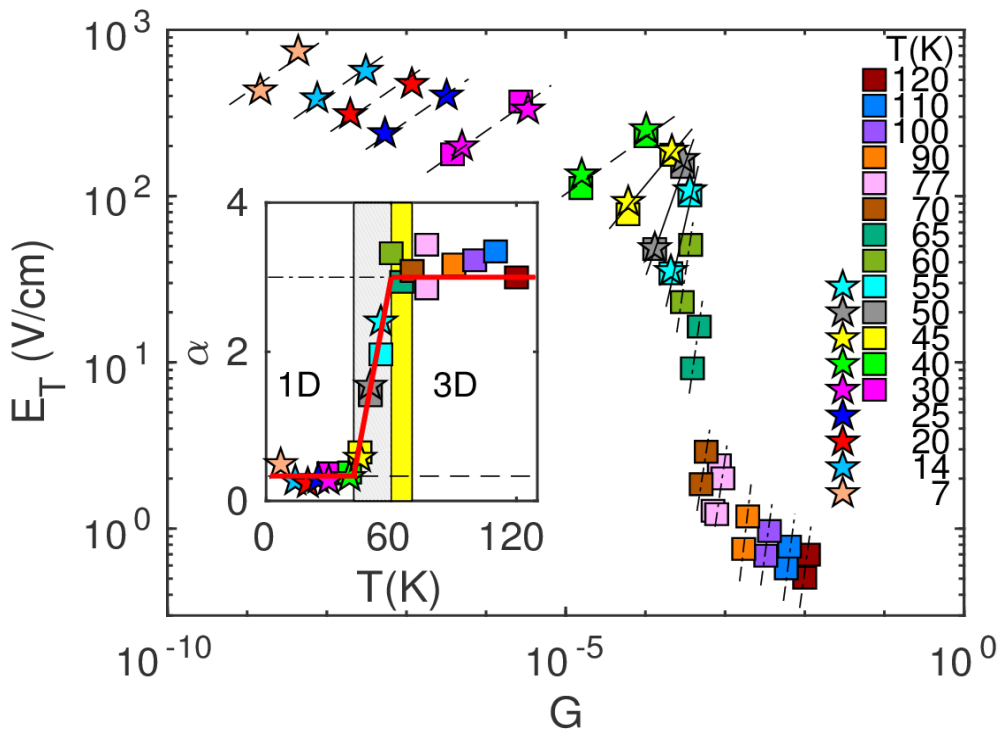


Fig. 7. Dependences of $E_{T,A,B}$ (squares) и $E_{T,A,B}^*$ (stars) on the corresponding normalized Ohmic conductances G at different T [18]. The inset shows the dependence of the exponent α on T . In the gray zone, the type of CDW pinning changes. In the yellow zone there is a sharp increase in $E_T(T)$.

At high T , quasiparticles excited over the Peierls gap dominate, and it is they that participate in screening the potential created by CDW deformation, providing 3D CDW pinning. The crystal under study is bulky ($S = 3.0 \mu\text{m}^2$), so the CDW pinning in it at $T \gtrsim 60$ K is three-dimensional [16]. With decreasing T , an increase in the concentration of excess solitons caused by strain leads to a change in the type of majority current

carriers. At $T \lesssim 45$ K, solitons dominate over quasiparticles, whose contribution decreases according to the activation law [12]. A change in the type of pinning with decreasing temperature means that the screening of electric fields caused by CDW deformation now has a 1D character, as in the case of very thin samples [8].

We also analyzed all previously obtained results of studying photoconduction in relatively thin samples of o -TaS₃ for a possible change in the CDW pinning dimensionality with increasing T . A summary picture, including the results of studies on samples of different cross-sections, is presented in Fig. 8. It was found that, in addition to the bulk sample, at least some of the thin samples show a transition from 1D to 3D pinning with increasing T without any strain. This may be since in these samples, one of the transverse sizes is larger than the CDW phase correlation length in this direction – the value of S for all samples was calculated from the resistance value at room temperature R_{300} . Thus, we observe a change in the CDW pinning dimensionality with a change in T in samples that differ in cross-sectional area by 2 orders of magnitude. This behavior appears to be a characteristic feature of o -TaS₃, associated with a change in the nature of the majority current carriers from single-particle to collective at low temperatures.

Conclusion

This work summarizes the results of a series of works devoted to the study of low-temperature conduction and photoconduction of the Peierls conductor o -TaS₃. The totality of the data obtained allows us to draw the following conclusions:

- 1) The difference in the conduction character of o -TaS₃ at high temperatures ($100 \lesssim T \lesssim 220$ K) and low temperatures ($T \lesssim 80$ K) is indeed due to the different nature of the majority current carriers. In the high-temperature region, it is carried out by single-particle carriers (quasiparticles), and in the low-temperature region, the predominant contribution is made by collective excitations (solitons). Conduction can be significantly increased due to photoconduction arising from nonequilibrium quasiparticles excited by illumination.

2) Similarly, the nature of photoconduction also differs at high $60 \lesssim T \lesssim 77$ K and low $T \lesssim 45$ K temperatures due to a change in the type of majority current carriers from single particle to collective. The collective contribution to low-temperature photoconduction, which is usually not noticeable, can be significantly enhanced by strain application, leading to an increase in the concentration of nonequilibrium collective carriers.

These statements are confirmed by the following fact. The CDW pinning dimensionality (established due to the discovered analogy between the effects of strain and illumination on the conduction of *o*-TaS₃) also changes dramatically with temperature, namely:

- 1) In the region of low temperatures ($T \lesssim 40$ K), one-dimensional (1D) CDW pinning is observed for all samples, including the bulk sample.
- 2) For some samples (including both a bulk sample and a few relatively thin samples), a transition from 1D to 3D CDW pinning is observed in a narrow temperature range of $40 \text{ K} \lesssim T \lesssim 60 \text{ K}$.

A decrease in the CDW pinning dimensionality with decreasing temperature is associated with a change in the screening conditions of electric fields arising during CDW deformation due to a change in the type of the main screening current carriers from single particle to collective carriers.

Financing: The research was carried out within the framework of the state assignment of the Kotelnikov IRE RAS No. 122042000064-1.

References

1. Monceau P., Electronic crystals: an experimental overview // Adv. Phys., 61, 325 (2012). <https://doi.org/10.1080/00018732.2012.719674>
2. Gruner G., The dynamics of charge-density waves // Rev. Mod. Phys. 60, 1129 (1988). <https://doi.org/10.1103/RevModPhys.60.1129>

3. Brasovskii S.A., Electronic excitation in the Peierls-Fröhlich state // Pis'ma v ZhETP 28, 656 (1978); [JETP Letters, 28, 606 (1978)].
http://jetpletters.ru/ps/1581/article_24247.pdf
4. Brazovskii S.A., Electronic excitations in the Peierls-Frolich state // Zh. Eksp. Teor. Fiz. 78, 677 (1980); // Sov. Phys. JETP 51, 342 (1980)]
https://doi.org/10.1142/9789814317344_0024
5. Brasovskii S., Brun C., Wang Z.-Z., Monceau P., Scanning-Tunneling Microscope Imaging of Single-Electron Solitons in a Material with Incommensurate Charge-Density Waves // Phys. Rev. Lett., 108, 096801. (2012).
<https://doi.org/10.1103/PhysRevLett.108.096801>
6. Latyshev Yu.I., Monceau P., Brasovskii S., Orlov A.P., Fournier T., Observation of Charge Density Wave Solitons in Overlapping Tunnel Junctions // Phys. Rev. Lett., 95, 266402 (2005). <https://doi.org/10.1103/PhysRevLett.95.266402>
7. Takoshima T., Ido M., Tsutsumi T., Sambongi T., Honma S., Yamaya K., Abe Y., Non-Ohmic conductivity of TaS₃ in the low-temperature semiconducting regime // Sol. State Commun., 35, 911 (1980).
[https://doi.org/10.1016/0038-1098\(80\)90987-4](https://doi.org/10.1016/0038-1098(80)90987-4)
8. Zaitsev-Zotov S.V., Minakova V.E., Photoconduction and photocontrolled collective effects in the Peierls conductor TaS₃ // Pis'ma v ZhETP, 79, 680 (2004).
<https://doi.org/10.1134/1.1787104>
9. Zybtssev S.G., Pokrovskii V.Ya, Strain-induced formation of ultra-coherent CDW in quasi one-dimensional conductors // Physica B 460, 34 (2015).
<https://doi.org/10.1016/j.physb.2014.11.035>
10. Wang Z.-Z., Salva H., Monceau P., Renard M., Roucau C., Ayroles R., Levy F., Guemas L., Meerschaut A., Incommensurate-commensurate transition in TaS₃ // J. Phys.-Lett., 44, L311 (1983). <https://doi.org/10.1051/jphyslet:01983004408031100>
11. Inagaki K., Tsubota M., Higashiyama K., Ichimua K., Tanda A., Yamamoto K., Hanasaki N., Ikeda N., Nogami Y., Ito T., Toyokawa H., Field-Induced Discommensuration in Charge Density Waves in *o*-TaS₃ // J. Phys. Sos. Jpn., 77, 093708 (2008). <https://doi.org/10.1143/JPSJ.77.093708>

12. Zaitsev-Zotov S.V., Minakova V.E., Evidence of Collective Charge Transport in the Ohmic Regime of o -TaS₃ in the Charge-Density-Wave State by a Photoconduction Study // Rev. Lett., 97, 266404 (2006). <https://doi.org/10.1103/PhysRevLett.97.266404>
13. Itkis M.E., Nad' F.Ya., Fundamental absorption edge of the Peierls insulator of orthorhombic tantalum trisulfide // JETP Letters 39, 373 (1984). http://jetpletters.ru/ps/1300/article_19642.pdf
14. Nasretdinova V.F., Zaitsev-Zotov S.V., Electric-field-dependent energy structure of quasi-one-dimensional conductor o -TaS₃ // JETP Lett., 89, 514 (2009). <https://doi.org/10.1134/S0021364009100099>
15. Ogawa N., Shiraga A., Kondo R., Kagoshima S., Miyano K., Photocontrol of Dynamic Phase Transition in the Charge-Density Wave Material K_{0.3}MoO₃ // Phys. Rev. Lett., 87, 256401 (2001). <https://doi.org/10.1103/PhysRevLett.87.256401>
16. Zaitsev-Zotov S.V., Finite-size effects in quasi-one-dimensional conductors with a charge-density wave // Physics – Uspekhi, 47, 533 (2004). <https://doi.org/10.1070/PU2004v047n06ABEH001675>
17. Zaitsev-Zotov S.V., Minakova V.E., Photoconduction and photocontrolled collective phenomena in Peierls conductor TaS₃ // J. Phys. IV 131 95 (2005). <https://doi.org/10.1051/jp4:2005131021>
18. Minakova V.E., Taldenkov A.N., S. V. Zaitsev-Zotov S.V., Soliton Photoconduction in the Charge-Density-Wave Conductor Orthorhombic TaS₃ // JETP Letters, 110, 178 (2019). <https://doi.org/10.1134/S0021364019150037>
19. Preobrazhensky V. B, Taldenkov A. N., Kal'nova I.Yu., Electrical conductivity of the uniaxially strained quasi-one-dimensional Peierls insulator TaS₃ // JETP Letters, 40, 944 (1984). http://jetpletters.ru/ps/1256/article_18987.pdf
20. Lear R. S, Skove M.J., Stillwell E.P., Brill J.W., Stress dependence of the charge-density-wave transitions in NbSe₃ and o -TaS₃ // Phys.Rev. B 29, 5656 (1984). <https://doi.org/10.1103/PhysRevB.29.5656>

21. Minakova V.E., Nasretdinova V.F., Zaitsev-Zotov S.V., Charge-density waves physics revealed by photoconduction // B: Condensed Matter, 460,185 (2015).
<https://doi.org/10.1016/j.physb.2014.11.064>
22. Ogawa N., Miyano K., Brazovskii S.A., Optical excitation in the creep phase of plastic charge-density waves // Phys. Rev. B 71, 075118 (2005).
<https://doi.org/10.1103/PhysRevB.71.075118>

For citation:

Minakova V.E., Zaitsev-Zotov S.V. Collective nature of low-temperature photoconduction and conduction in Peierls conductor orthorhombic TaS₃. // Journal of Radio Electronics. – 2023. – №. 12. <https://doi.org/10.30898/1684-1719.2023.12.17>